Inorganic Chemistry

Forum Article

pubs.acs.org/IC

Reaction Mechanisms of Small-Molecule Activation by Amidoditetrylynes $R_2N-EE-NR_2$ (E = Si, Ge, Sn)

Markus Hermann,[†] Cameron Jones,*[,‡] and Gernot Frenking*[,†]

[†]Fachbereich Chemie, Philipps-Universität Marburg, 35032 Marburg, Germany

[‡]Monash University, P.O. Box 23, Melbourne, Victoria 3800, Australia

ABSTRACT: The calculated reaction profiles using density functional theory at the BP86/TZVPP level for the reaction of small molecules with amidoditetrylynes $R_2N-EE-NR_2$ (E = Si, Ge, Sn) are discussed. Four projects are presented that feature the virtue of cooperation between theory and experiment. First, the calculated reaction paths for hydrogenation of the model systems $(Me_2N)EEL(NMe_2)$ (E = Si, Ge, Sn), which possess E−E single bonds, are examined. The results for the germanium model systems are compared with hydrogenation of the real system $L^{\dagger}GeGeL^{\dagger}$ where $L^{\dagger}$ = NAr*(SiMe$_3$) (Ar* = $C_6H_2\{C(H)Ph_2\}_2Me$-2,6,4). The second project introduced the multiply bonded amidodigermyne $L^{\dagger\dagger}GeGeL^{\dagger\dagger}$, which carries the extremely bulky substituents $L^{\dagger\dagger}$ = N(Ar††)(SiPr$^i_3$), where Ar†† = $C_6H_2\{C(H)Ph_2\}_2Pr^i$-2,6,4. The theoretical reaction profile for dihydrogen addition to $L^{\dagger\dagger}GeGeL^{\dagger\dagger}$ is discussed. Hydrogenation gives $L^{\dagger\dagger}(H)GeGe(H)L^{\dagger\dagger}$ as the product, which is in equilibrium with the hydrido species $Ge(H)L^{\dagger\dagger}$. The latter germanium hydride and tin homologue $Sn(H)L^{\dagger\dagger}$ were found to be effective catalysts for hydroboration reactions, which is the topic of the third project. Finally, the calculated reaction course for the reduction of CO_2 to CO with the amidodigermyne $L^{\dagger}GeGeL^{\dagger}$ is discussed.

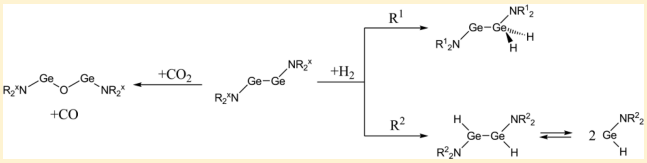

1. INTRODUCTION

Fundamental advances have been made in the chemistry of low-oxidation-state p-block compounds in the last 2 decades, during which isolation of a large number of molecules with unusual bonding motifs and astonishing reactivities was achieved.[1] The remarkable progress in the field of low-coordinated main-group chemistry is an example for modern chemical research where theory and experiment mutually stimulate and support each other in an exemplary way. A striking example for cooperation between theoretical and experimental research is provided by recent work where heavy group 14 homologues of alkynes LEEL (E = Ge, Sn) were used for the activation of small substrate molecules.[2] Isolation and structural characterization of the complete set of group 14 ditetrylynes LEEL (E = Si−Pb), which have bulky aryl or silyl groups L, were achieved between 2000 and 2004 by Power et al.[3] (E = Ge−Pb) and Sekiguchi et al.[4] (E = Si). Several theoretical studies[5] analyzed the bonding situation in the compounds, which exhibit a trans-bent geometry of the LEEL moiety with bending angles between ~94° (LPbPb)[3a] and 137° (LSiSi).[4a] It was shown that the unusual equilibrium geometries can be explained in terms of interactions between the fragments EL in the electronic ground state.[5b]

The interest in ditetrylynes received a major boost in 2005 when Power et al. reported that the digermyne Ar$^{\#}$GeGeAr$^{\#}$ [Ar$^{\#}$ = $C_6H_3(C_6H_3Pr^i_2$-2,6)$_2$-2,6] activates dihydrogen (H_2) at room temperature and atmospheric pressure.[6] The reaction yielded mixtures of Ar$^{\#}$(H)GeGe(H)Ar$^{\#}$, Ar$^{\#}(H)_2$GeGe-$(H)_2$Ar$^{\#}$, and Ar$^{\#}GeH_3$, whose proportions depend on the reaction stoichiometry. The hydrogenation reaction of the analogous distannyne Ar$^{\#}$SnSnAr$^{\#}$ gave the doubly bridged Ar$^{\#}$Sn(μ-H)$_2$SnAr$^{\#}$.[7] The experimental results indicated that the steric properties of L in ditetrylynes LEEL have a distinct influence on the reaction course. The mechanism of the addition of H_2 to the digermyne Ar$^{\#}$GeGeAr$^{\#}$ and the distannyne Ar$^{\#}$SnSnAr$^{\#}$ was investigated in a detailed theoretical study by Wang, Schleyer, and co-workers.[8]

The bonding situation and chemical behavior of LEEL is determined not only by steric factors but also by the electronic properties of L. The influence of the steric and electronic effects of the ligands on the structure and reactivity of ditetrylynes is the topic of ongoing experimental and theoretical investigations by Jones, Frenking and co-workers.[9−14] The experimental findings revealed surprising and unexpected results. We found that the Ge−Ge bonding situation in the amidodigermynes $R^1R^2N-GeGe-NR^1R^2$ can be modulated from single to multiple bonding by the donor strength of the amido groups in conjunction with the steric bulk of the substituents R^1 and R^2.[13] This has a profound influence on the structure and reactivity of the molecules. Both singly and multiply bonded amidodigermynes activate H_2, but the reaction products are different.[10,11,13] Experimental evidence suggested that hydrogenation of amidodigermynes may lead to the formation of hydridogermylene $H-Ge-NR^1R^2$. Recent work reported that hydridogermylens and hydridostannylenes $H-Sn-NR^1R^2$ are effective catalysts for the hydroboration of carbonyl compounds.[14] Amidodigermynes $R^1R^2N-GeGe-NR^1R^2$ also react with CO_2 under mild conditions.[9] Thus, amidoditetrylynes are versatile compounds

Special Issue: Insights into Spectroscopy and Reactivity from Electronic Structure Theory

Received: February 26, 2014
Published: May 5, 2014

dx.doi.org/10.1021/ic500457q | Inorg. Chem. 2014, 53, 6482−6490

that may be employed for a variety of small-molecule activations. In this Forum Article, we summarize the theoretical studies of the reaction mechanisms of the activation of small molecules by amidoditetrylynes that have been obtained so far.[9,11−14]

2. METHODS

The computational details used in the studies summarized herein are given in the original publications, which are cited appropriately throughout the main text. Therefore, we give only a brief account of the methods. The geometry optimizations were carried out with the *Gaussian 09* optimizer[15] in conjunction with *Turbomole 6.4*[16] energies and gradients at the BP86 level[17] of theory using def2-TZVPP[18] and def2-SVP[19] basis sets. The tin atom was calculated with a quasi-relativistic effective core potential.[20] Stationary points were characterized by calculating the Hessian matrix analytically. Thermal corrections have been taken from these calculations. All energies in this manuscript are ΔG values at 298 K. The effect of dispersion interactions has been estimated in some projects using Grimme et al.'s D3 term.[21] Solvent effects were considered by calculations with the COSMO model by Klamt et al.[22] The orbital interactions at the transition state between H_2 and L′GeGeL′ (**1Ge′**) have been investigated with the EDA−NOCV method,[23] which combines energy decomposition analysis (EDA)[24] and the natural orbitals for chemical valence (NOCV).[25] The EDA−NOCV calculations were carried out at BP86 using TZ2P+ basis sets[26] with the *ADF 2010.02b* program package.[27] Further calculations were carried out with the meta-hybrid functional M06-2x[28] using the program package *Orca*.[29]

3. HYDROGENATION REACTIONS

The starting point of our studies on the reactivity of ditetrylynes was the synthesis of the amidodigermyne $L^{\dagger}GeGeL^{\dagger}$ (**1Ge**), where $L^{\dagger}$ = NAr*(SiMe$_3$) (Ar* = $C_6H_2\{C(H)Ph_2\}_2$Me-2,6,4), and its reaction with H_2.[9] Theoretical analysis showed that the Ge−Ge bond in **1Ge**, which is significantly longer (2.709 Å) than that in $Ar^{\#}GeGeAr^{\#}$ (2.285 Å)[6] [$Ar^{\#}$ = $C_6H_3(C_6H_3Pr^i_2$-2,6)$_2$-2,6], should be classified as a single bond and that the dicoordinated germanium atoms of **1Ge** each possess a lone pair of electrons. The N → Ge π donation into the formally vacant p(π) atomic orbital of germanium stabilizes the digermyne **1Ge** in an unprecedented way.

Scheme 1 summarizes the results of the hydrogenation reaction of **1Ge**, which takes place at room temperature and under normal pressure. The only product that could be isolated is the singly hydrogenated mixed-valence compound $L^{\dagger}GeGe(H)_2L^{\dagger}$.[9] NMR spectroscopic data showed that the symmetrical product $L^{\dagger}(H)GeGe(H)L^{\dagger}$ was in equilibrium with $L^{\dagger}GeGe(H_2)L^{\dagger}$ in solution, while the doubly hydrogenated species $L^{\dagger}Ge(H)_2Ge(H)_2L^{\dagger}$ was not observed. The mechanism of the hydrogenation reaction of **1Ge** and related silicon and tin homologues was analyzed in a following theoretical work.[12]

Scheme 1. Synthesis of the Singly Bonded Amidodigermyne 1Ge and the Hydrogenation Product $L^{\dagger}GeGe(H)_2L^{\dagger}$ (3Ge; ^{Mes}Nacnac = $[(MesNCMe)_2CH]^-$, Mes = mesityl).[9]

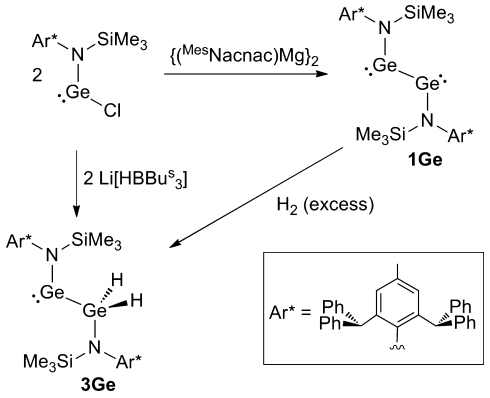

Figure 1 shows the calculated reaction profile for H_2 addition to the model digermyne **1Ge′**, where the bulky substituents $L^{\dagger}$ of **1Ge** are replaced by L′ = NMe_2. The rate-determining initial reaction, which is mildly exergonic (ΔG°_{298} = −1.0 kcal/mol), leads to the singly hydrogen-bridged species **2Ge′**, which rearranges in two separate reactions with very small barriers to the energetically lower-lying asymmetrical species **3Ge′** and the symmetrical compound **4Ge′**. Further hydrogenation toward the fully hydrogenated compound **5Ge′** or toward the products **6Ge′** + **7Ge′**, which proceeds with rupture of the Ge−Ge bond, has clearly higher activation barriers than the first hydrogenation step ($\Delta G^{\circ\ddagger}_{298}$ = 20.8 kcal/mol). Note that the activation barriers for the second hydrogenation must be calculated with respect to the energy of **3Ge′**.

The calculations thus suggest a rapid equilibration between the isomers **3Ge′** ⇄ **2Ge′** ⇄ **4Ge′**, with **3Ge′** as the most stable form and **4Ge′** being slightly higher in energy. This is in agreement with the experimental results of the real system **1Ge**, where only the 1,1-form $LGeGe(H)_2L$ (**3Ge**) was isolated as the reaction product in the solid state but the symmetrical isomer LGe(H)Ge(H)L (**4Ge**) could be observed by NMR spectroscopy.[9] The very large activation barriers for the second hydrogenation ($\Delta G^{\circ\ddagger}_{298}$ = 29.8 kcal/mol) and for the hydrogenation with concomitant Ge−Ge bond fission ($\Delta G^{\circ\ddagger}_{298}$ = 32.0 kcal/mol) make it understandable that these reactions are not observed.

In order to find out whether the results for the model digermyne **1Ge′** are valid for the real compound **1Ge**, the authors calculated also the reaction profile for the hydrogenation reaction of **1Ge**. The results are shown in Figure 2.

The comparison of the free-energy profiles for H_2 addition to the real compound **1Ge** with hydrogenation of the model system **1Ge′** (Figure 1) shows that the essential features do not change very much. The first hydrogenation proceeds with initial formation of the singly hydrogen-bridged species **2Ge** and subsequent rearrangement toward the asymmetrical species **3Ge** that was isolated and the slightly less stable symmetrical compound **4Ge**, which was identified by NMR spectroscopy.[9] The only difference between the real system and model compound concerns the second hydrogenation step. Figure 2 shows that formation of the products **6Ge** + **7Ge** now has a lower barrier than formation of the fully hydrogenated compound **5Ge**. However, the addition of a second H_2 still has much higher barrier than the addition of the first H_2. The calculated results, which consider solvent effects (numbers in italics) and the dispersion forces (bold numbers), do not change the conclusion of the theoretical study, which provides an understanding of the experimental observations.

Calculations have also been carried out for the hydrogenation reactions of the corresponding silicon and tin homologues of the model systems **1Si′** and **1Sn′**. The theoretical reaction profiles are shown in Figures 3 and 4. The calculated reaction path for the silicon system **1Si′** (Figure 3) exhibits the same type of energy minima and transition states as those for **1Ge′** (Figure 1), but the activation barriers for silicon are lower and the reaction steps are more exergonic than those for

dx.doi.org/10.1021/ic500457q | Inorg. Chem. 2014, 53, 6482−6490

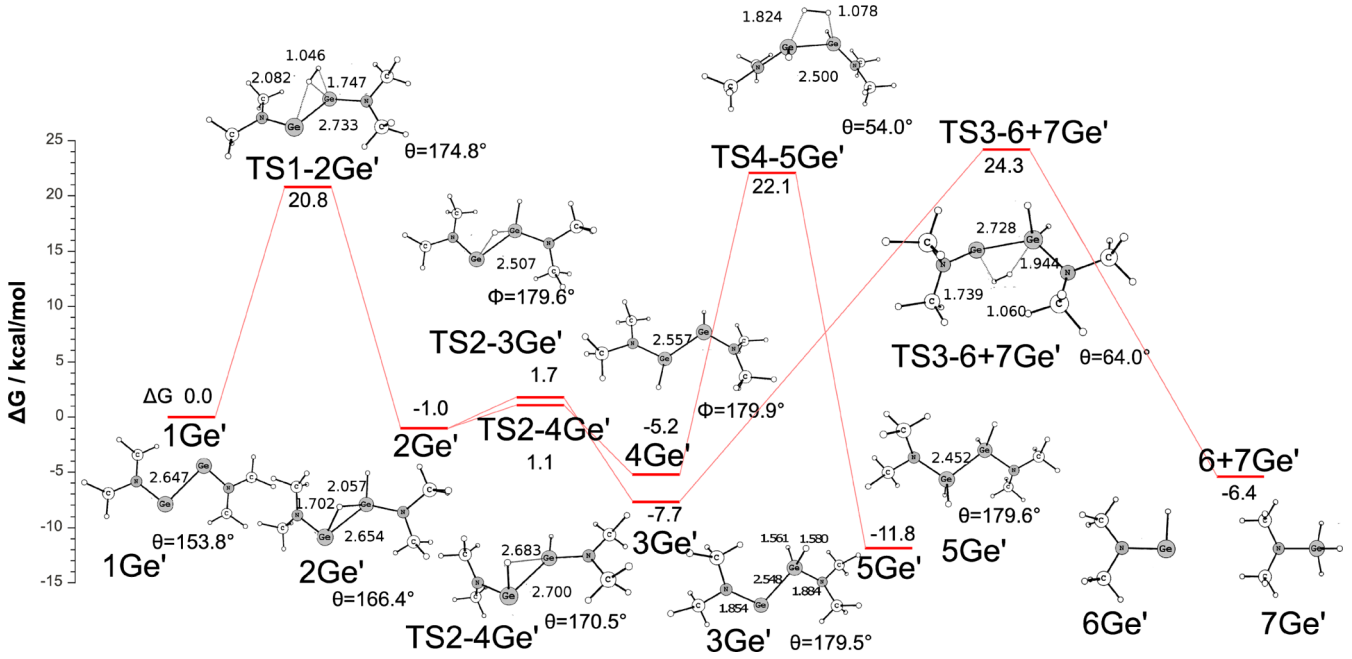

Figure 1. Calculated reaction profile for the addition of H_2 to the singly bonded amidodigermyne **1Ge′** with model substituents L′ at BP86/def2-TZVPP. Bond lengths are given in angstroms and angles in degrees. The dihedral angle θ refers to the NGeGeN fragment.[12]

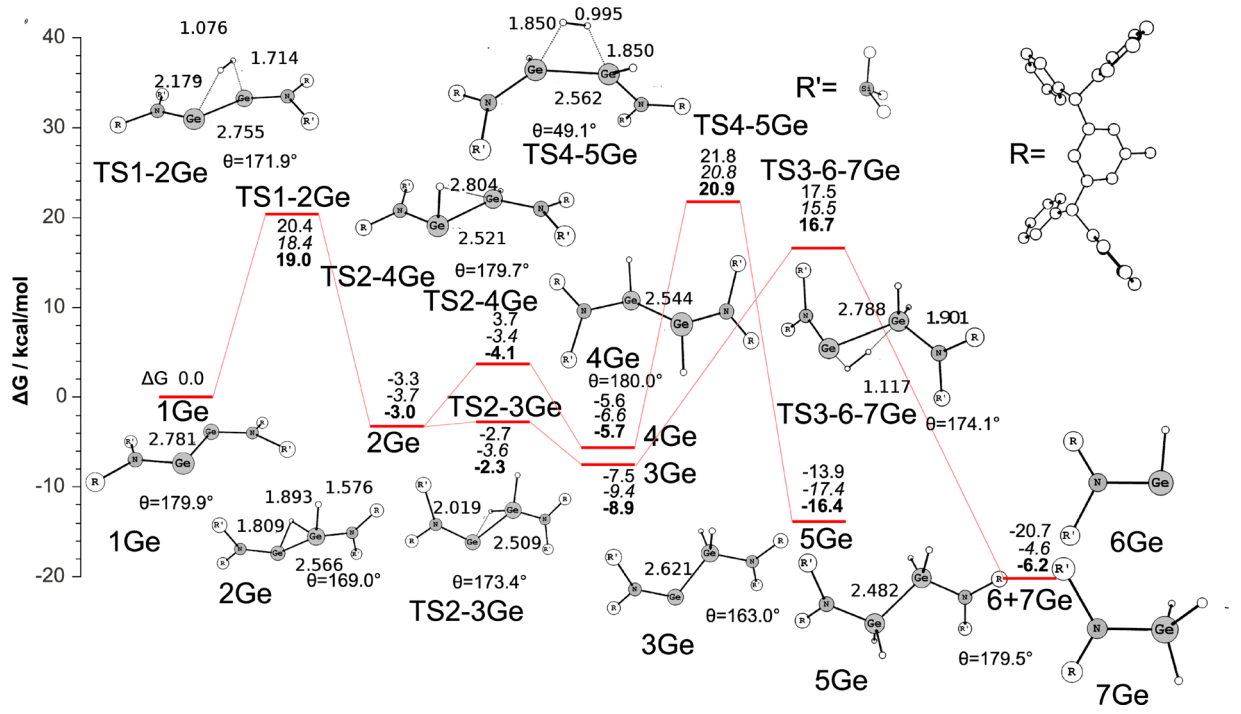

Figure 2. Calculated reaction profile for the addition of H_2 to the singly bonded amidodigermyne **1Ge** with real substituents L† at BP86/def2-TZVPP//BP86/def2-SVP. The values in italics include dispersion interactions, which were calculated at BP86/def2-TZVPP+D3//BP86/def2-SVP. The bold values consider solvent effects, which were calculated at BP86/def2-TZVPP+D3-COSMO//BP86/def2-SVP. Bond lengths are given in angstroms and angles in degrees. The dihedral angle θ refers to the NGeGeN fragment.[12]

germanium. The first hydrogenation step of **1Si′** leads first to the singly hydrogen-bridged species **2Si′**, which then rearranges toward the asymmetrical species **3Si′** and the slightly less stable symmetrical isomer **4Si′**. The activation barriers for the second hydrogenation, which is a thermodynamically favored process, are still higher ($\Delta G^{\circ\ddagger}_{298}$ = 19.2 kcal/mol for **5Si′** and $\Delta G^{\circ\ddagger}_{298}$ = 19.1 kcal/mol for **6Si′** + **7Si′**) than those for the first hydrogenation ($\Delta G^{\circ\ddagger}_{298}$ = 15.2 kcal/mol). However, the differences are not very large, which means that the silicon system might engage in full hydrogenation.

The calculated reaction profile for the tin system **1Sn′** introduces a novel species as the product of the first hydrogenation reaction, i.e., the doubly hydrogen-bridged compound **8Sn′** (Figure 4). A doubly bridged product $Ar^{\#}Sn(\mu\text{-}H)_2SnAr^{\#}$ has been observed in the hydrogenation reaction of $Ar^{\#}SnSnAr^{\#}$.[7] The calculations suggest that **8Sn′** is the

dx.doi.org/10.1021/ic500457q | Inorg. Chem. 2014, 53, 6482−6490

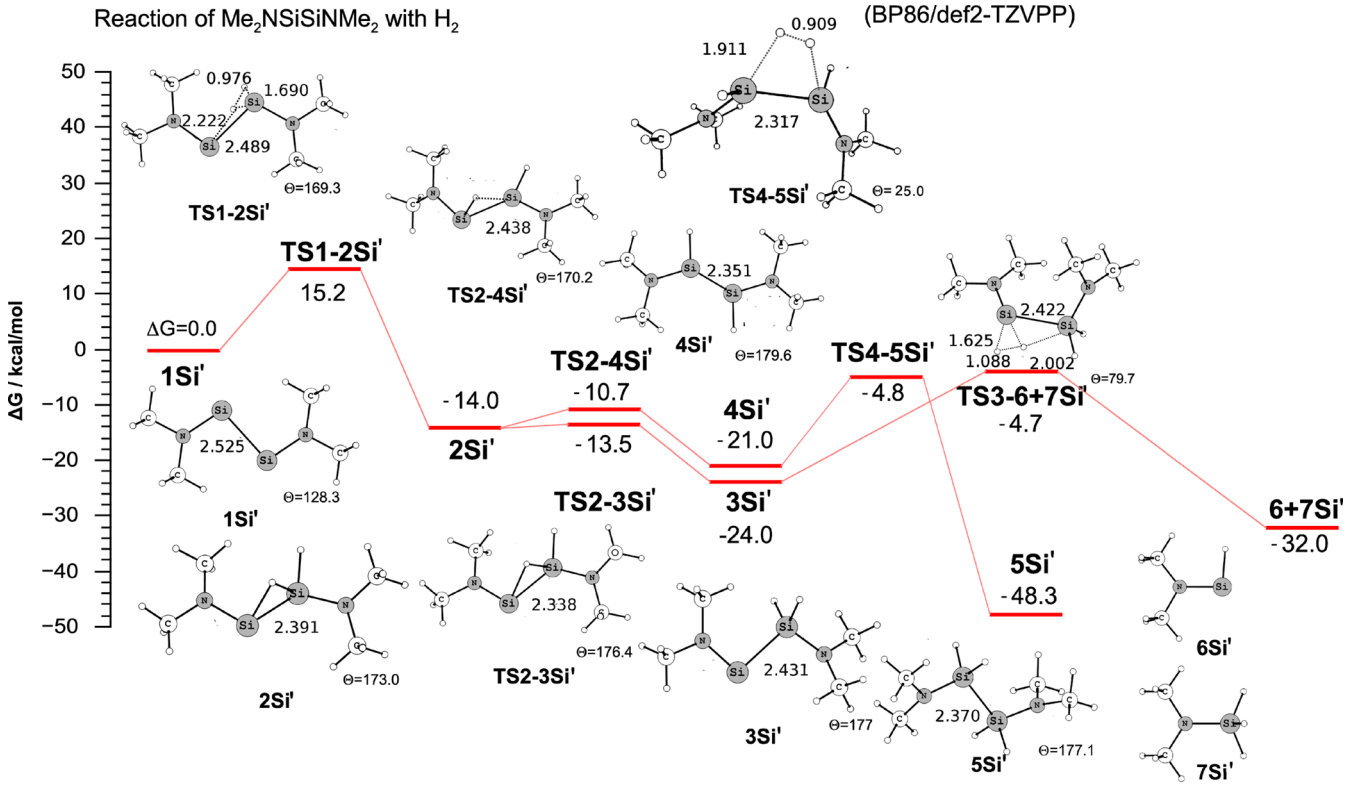

Figure 3. Calculated reaction profile for the addition of H_2 to the singly bonded amidodisilylyne L′SiSiL′ with model substituents L′ (**1Si′**) at BP86/def2-TZVPP. Bond lengths are given in angstroms and angles in degrees. The dihedral angle θ refers to the NSiSiN fragment.[12]

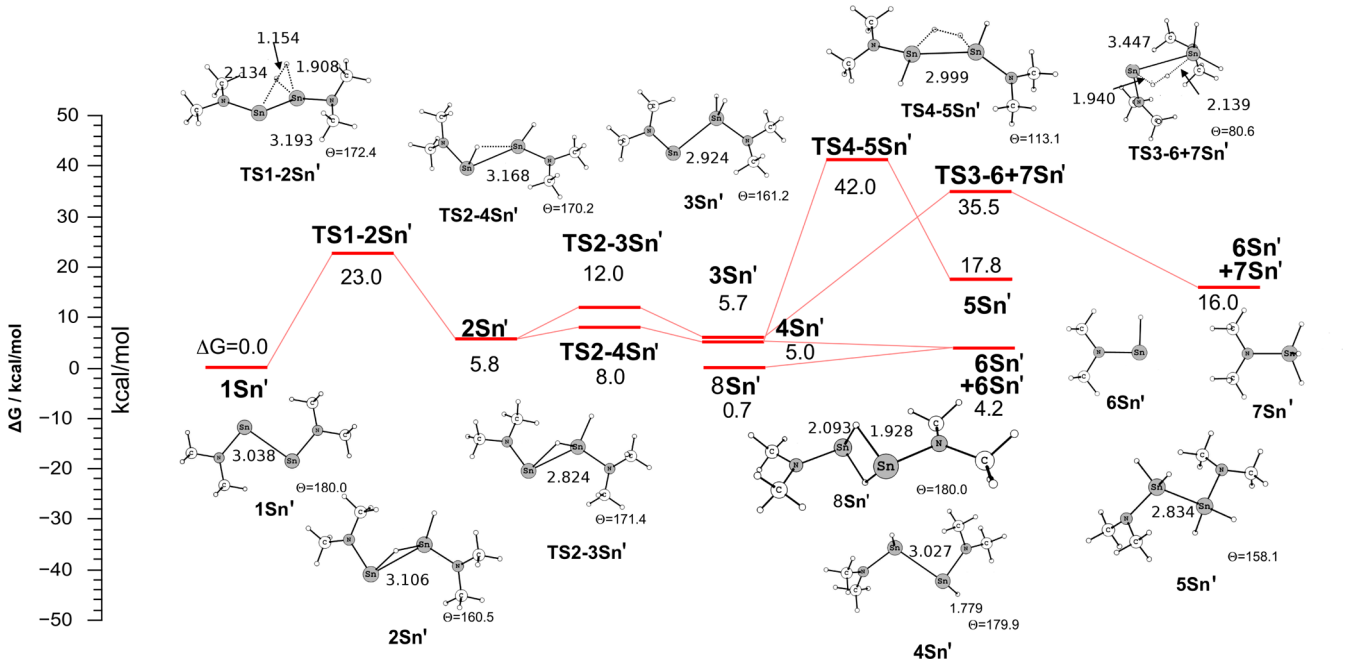

Figure 4. Calculated reaction profile for the addition of H_2 to the singly bonded amidodistannyne L′SnSnL′ with model substituents L′ (**1Sn′**) at BP86/def2-TZVPP. Bond lengths are given in angstroms and angles in degrees. The dihedral angle θ refers to the NSnSnN fragment.[12]

energetically lowest-lying isomer of the first hydrogenation of **1Sn′** with the symmetrical form **4Sn′** and the asymmetrical form **3Sn′** coming next. The overall hydrogenation of the tin compound **1Sn′** is predicted to be kinetically and thermodynamically less favored than H_2 addition to the germanium and silicon homologues. The calculated activation barriers and reaction energies for the amidoditetrylynes are shown in Table 1. The data establish a reactivity ordering of the three group 14 atoms to be Si > Ge > Sn.

We also analyzed the orbital interactions in the transition state **TS1-2Ge′** of the initial H_2 addition to **1Ge′** (Figure 1) using the EDA−NOCV method.[23] Figure 5 shows the most important results. The question that was addressed concerns the strength of the highest occupied molecular orbital

dx.doi.org/10.1021/ic500457q | Inorg. Chem. 2014, 53, 6482−6490

Table 1. Calculated Activation Energies $\Delta\hat{G}^{\ddagger}$ and Reaction Energies ΔG_R at BP86/def2-TZVPP (kcal/mol) of the Most Important Steps of Hydrogenation of L′EEL′ and 1Ge

		E = Si	E = Ge[a]	E = Sn
1E′ + H_2 → 2E′	$\Delta G^{\ddagger}$	15.2	20.8 (20.4, 18.4, **19.0**)	23.0
	ΔG_R	−14.0	−1.0 (−3.3, −3.7, **−3.0**)	5.8
3E′ + H_2 → → → 5E′	$\Delta G^{\ddagger}$	19.2	29.8 (29.3, 30.2, **29.8**)	41.3[b]
	ΔG_R	−24.3	−4.1 (−6.4, *−8.0*, **7.5**)	17.1[b]
3E′ + H_2 → 6E′ + 7E′	$\Delta G^{\ddagger}$	19.3	32.0 (25.0, 24.9, **25.6**)	34.8
	ΔG_R	−8.0	1.3 (−13.2, 4.8, **2.7**)	15.3

[a]The values in parentheses refer to the real system **1Ge** and were calculated at BP86/def2-TZVPP//BP86/def2-SVP. The data in italics include dispersion interactions at BP86/def2-TZVPP+D3//BP86/def2-SVP. The bold values consider also solvent effects at BP86/def2-TZVPP+D3-COSMO//BP86/def2-SVP. [b]Values for the reaction of **8Sn**′.

(HOMO)−lowest unoccupied molecular orbital (LUMO) interactions between the two reactants H_2 and **1Ge**′. Figure 5b shows the shape of the frontier orbitals of the reactants. Figure 5 displays the results of the EDA−NOCV calculations in terms of HOMO(H_2) → LUMO(**1Ge**′) donation and LUMO(H_2) ← HOMO(**1Ge**′) back-donation. The green and yellow regions denote the areas of charge donation (yellow) and charge acceptance (green), and the calculated energy values indicate the strength of the respective orbital interactions. It becomes obvious that charge donation from H_2 to **1Ge**′ ($\Delta E_{orb}' = -37.0$ kcal/mol) occurs mainly to the germanium atom at the right-hand side. The slightly weaker back-donation in the opposite direction ($\Delta E_{orb}'' = -35.1$ kcal/mol) is mainly associated with charge accumulation between the bridging hydrogen atoms and the germanium atom at the left-hand side.

Analysis of the electronic structure of the amidodigermyne **1Ge** clearly showed that the germanium atoms carries lone electron pairs and that the formally vacant p(π) atomic orbital of germanium receives electronic charge through N → Ge π donation, while the Ge−Ge π-bonding orbital is vacant. The compound has a long Ge−Ge bond (2.709 Å) and an obtuse bending angle N−Ge−Ge of 100.1°,[9] which is typical of singly bonded LEEL species (E = Si−Pb).[5b,d] If structural conditions would diminish or prevent N → Ge π donation, one could expect a change in the bonding situation toward a multiply bonded compound. This was indeed achieved with synthesis of the amidodigermyne $L^{\dagger\dagger}$GeGe$L^{\dagger\dagger}$ (**1Ge**††), which carries the extremely bulky substituents $L^{\dagger\dagger}$ = N($Ar^{\dagger\dagger}$)($SiPr^i_3$), where $Ar^{\dagger\dagger}$ = $C_6H_2\{C(H)Ph_2\}_2Pr^i$-2,6,4.[13] Steric repulsion between the substituents $L^{\dagger\dagger}$ leads to a rotation of the amido groups out of the NGeGeN plane, which reduces N → Ge π donation to such an extent that the π-bonding orbital, which is the LUMO in **1Ge**, becomes the HOMO in **1Ge**††. The different bonding situation manifests itself in the geometry of **1Ge**††, which has a much shorter Ge−Ge bond of 2.357 Å and a more obtuse bending angle N−Ge−Ge of 120.4° than those in **1Ge**.[13]

The multiply bonded digermyne **1Ge**†† reacts with H_2 and showed a markedly different behavior compared with the singly bonded **1Ge**. The compound activates H_2 below 0 °C in a hydrogenation reaction, which leads to the symmetric hydridodigermene $L^{\dagger\dagger}$(H)GeGe(H)$L^{\dagger\dagger}$. The asymmetric species $L^{\dagger\dagger}$GeGe$(H)_2L^{\dagger\dagger}$ was not observed. Spectroscopic and theoretical evidence indicate that $L^{\dagger\dagger}$(H)GeGe(H)$L^{\dagger\dagger}$ exists in equilibrium with the hydridogermylene :Ge(H)($L^{\dagger\dagger}$) in solution.[13]

Figure 6 shows the calculated reaction profile for the addition of H_2 to **1Ge**††.[13] The overall reaction path is not very different from the hydrogenation reaction of **1Ge** (Figure 2) with two notable differences. One difference is the lower activation barrier

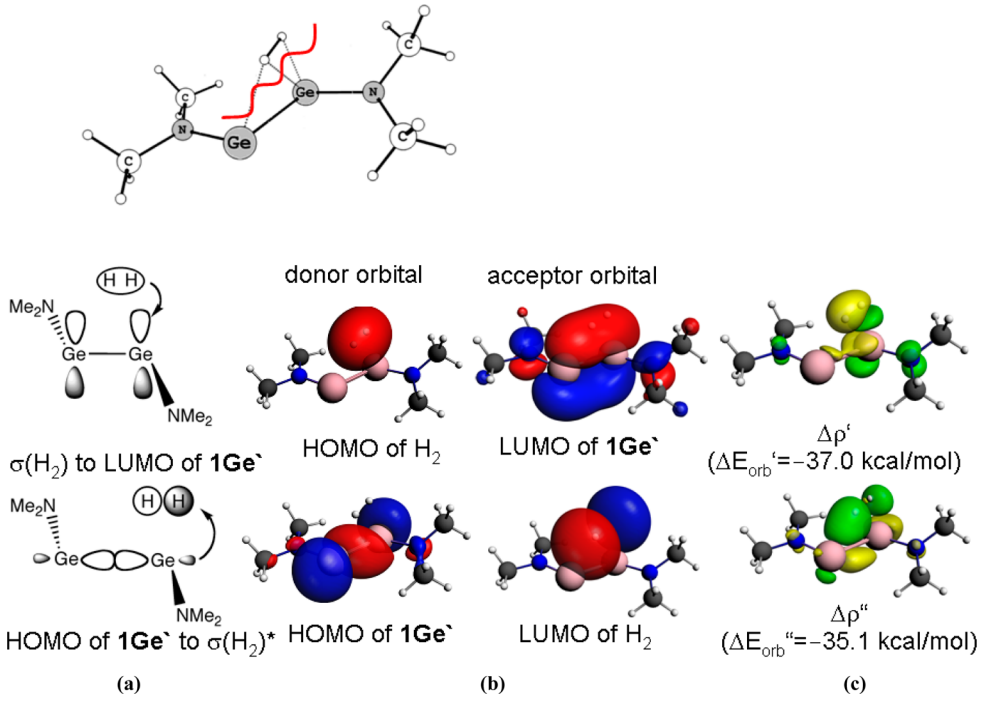

Figure 5. EDA−NOCV analysis of the transition state **TS1-2Ge**′. (a) Qualitative sketch of the orbital interactions between H_2 and Me_2N−GeGe−NMe_2 (**1Ge**′). (b) Frontier orbitals of the reacting species H_2 and **1Ge**′. (c) EDA−NOCV stabilization energies between the two most important pairs of interacting orbitals in the transition state **TS1-2Ge**′. The deformation densities $\Delta\rho'$ and $\Delta\rho''$ give the charge flow from the yellow to green areas.[12]

dx.doi.org/10.1021/ic500457q | Inorg. Chem. 2014, 53, 6482−6490

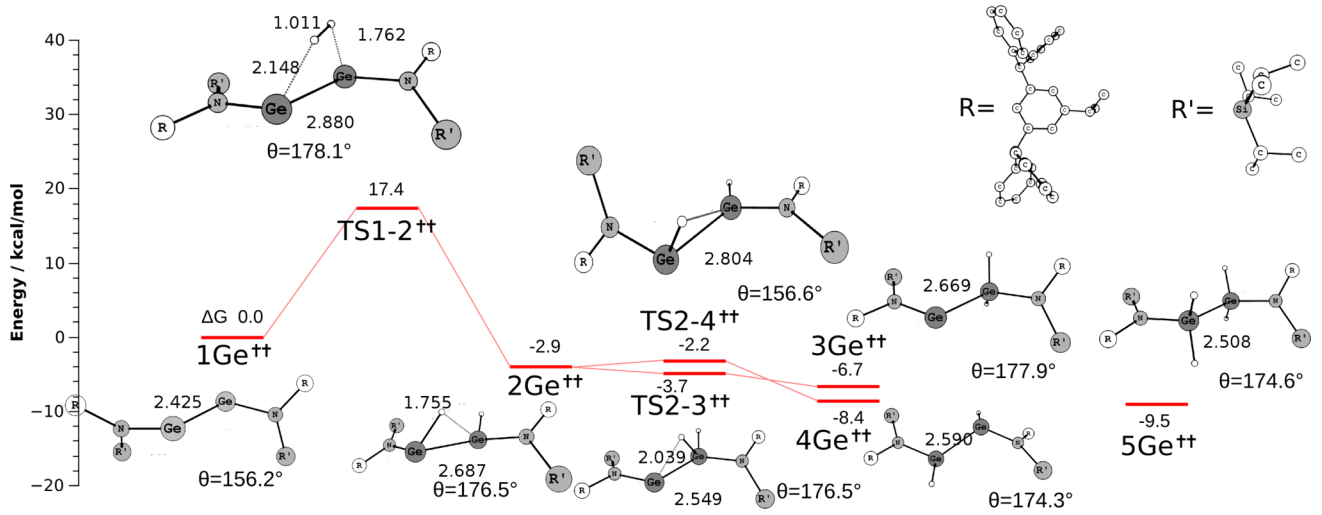

Figure 6. Calculated reaction profile for the addition of H_2 to the multiply bonded amidodigermyne with real substituents $L^{\dagger\dagger}$ (**1Ge**††) at BP86/def2-TZVPP//BP86/def2-SVP. Bond lengths are given in angstroms and angles in degrees. The dihedral angle θ refers to the NGeGeN fragment.[13]

for the entrance reaction of **1Ge**†† ($\Delta G^{\circ\ddagger}_{298}$ = 17.4 kcal/mol) than that for **1Ge** ($\Delta G^{\circ\ddagger}_{298}$ = 20.4 kcal/mol). The second difference is the finding that the symmetric isomer of the hydrogenated product **4Ge**†† is more stable than the asymmetric form **3Ge**††, which concurs with experiment. The transition state for the further hydrogenation toward **5Ge**†† could not be located. Calculations suggest that the latter step is only mildly exergonic by −1.1 kcal/mol.[13]

An important question concerns the experimentally observed equilibrium $L^{\dagger\dagger}$(H)GeGe(H)$L^{\dagger\dagger}$ (**4Ge**††) ⇄ 2$L^{\dagger\dagger}$(H)Ge (**6Ge**††). Calculations at BP86+D3/def2-TZVPP, which consider dispersion interactions using Grimme et al.'s D3 term,[21] suggest that the dissociation is endergonic by 19.4 kcal/mol.[13] The consideration of solvent effects with the COSMO[22] model lowers the value to 16.1 kcal/mol, which is still too high to explain the experimentally observed occurrence of the hydridogermylene $L^{\dagger\dagger}$(H)Ge (**6Ge**††). Experimental studies were also carried out aimed at the synthesis of the analogous tin compound **4Sn**††, which gave a doubly hydrogen-bridged valence isomer [$L^{\dagger\dagger}$Sn(μ-H)]$_2$ (**8Sn**††) instead of the anticipated product. The analogous germanium species **8Ge**†† is energetically higher-lying than the classical isomers **3Ge**†† and **4Ge**†† and, therefore, it is not shown in Figure 6. The NMR spectroscopic data suggest that **8Sn**†† also partially dissociates into the hydridostannylene $L^{\dagger\dagger}$(H)Sn (**6Sn**††).[13] Calculations at the BP86+D3/def2-TZVPP level give a free dissociation energy of 15.4 kcal/mol, which again is too high.

Inspection of the calculated data and further calculations suggest that the discrepancy between theory and experiment may come from the estimate of the dispersion interactions. The calculated free energy ΔG°_{298} for the equilibrium **4Ge**†† ⇄ 2 **6Ge**†† at BP86/def2-TZVPP is −10.5 kcal/mol, while the calculated value for the equilibrium **8Sn**†† ⇄ 2 **6Sn**†† at this level is −8.2 kcal/mol. This means that dissociation into the monomers is clearly favored when dispersion forces are ignored. Calculations of the small model systems Me_2N−MM−NMe_2 and Me_2N−M (M = Ge, Sn) at different levels of theory showed that the theoretically predicted strength of the M−M bond at BP86/def2-TZVPP (−14.0 kcal/mol) is not very different from the calculated value at M06-2x/def2-TZVPP (−13.2 kcal/mol). The latter meta-hybrid functional intrinsically includes dispersion interactions.[28] The free energy ΔG°_{298} for the equilibrium **4Ge**†† ⇄ 2 **6Ge**†† at M06-2x/def2-TZVPP is 9.2 kcal/mol. The calculated equilibrium **8Sn**†† ⇄ 2 **6Sn**†† at this level is 4.9 kcal/mol. The latter values are much more favorable than the BP86+D3/def2-TZVPP results. We are currently investigating the strength of dispersion interactions on the latter reactions using various methods.

4. HYDROBORATION

The finding that the germanium and tin hydrido complexes $L^{\dagger\dagger}$(H)M (M = Ge, Sn), which have a formally empty p(π) orbital at atom M, are present in solution paved the way for a new area in the field of low-coordinated group 14 compounds. The complexes **6Ge**†† and **6Sn**†† were successfully employed by Hadlington et al. as efficient catalysts for the hydroboration of carbonyl compounds.[14] The mechanistic studies were supported by quantum-chemical calculations of the reaction courses. The proposed cycle for the hydroboration of R^1R^2CO (R^1/R^2 = alkyl, aryl, H) with the borane reagent HBpin (pin = pinacolato) catalyzed by $L^{\dagger\dagger}$(H)M is shown in Scheme 2.

Scheme 2. Proposed Cycle for the Hydroboration of Carbonyl Compounds (R^1)(R^2)CO (R^1/R^2 = Alkyl, Aryl, H) Using $L^{\dagger\dagger}$MH [M = Ge (6Ge**††), Sn (**6Sn**††)] as Catalysts[14]**

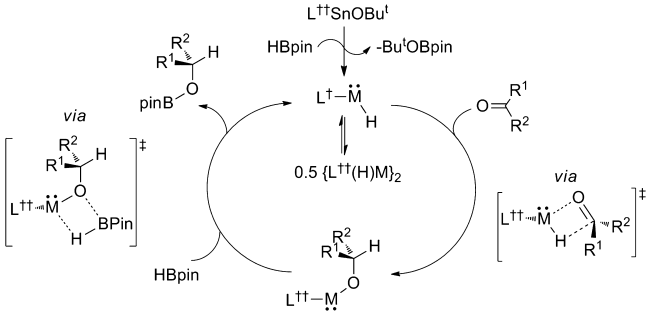

Figures 7 and 8 show the calculated profiles for the two-stage reaction of O=C(Pr^i)$_2$ with HBpin catalyzed by **6Ge**†† and **6Sn**††, respectively.

In the first step of the reaction of the hydride complexes **6M**†† undergoes a formal 2 + 2 addition of the M−H bond to

dx.doi.org/10.1021/ic500457q | Inorg. Chem. 2014, 53, 6482−6490

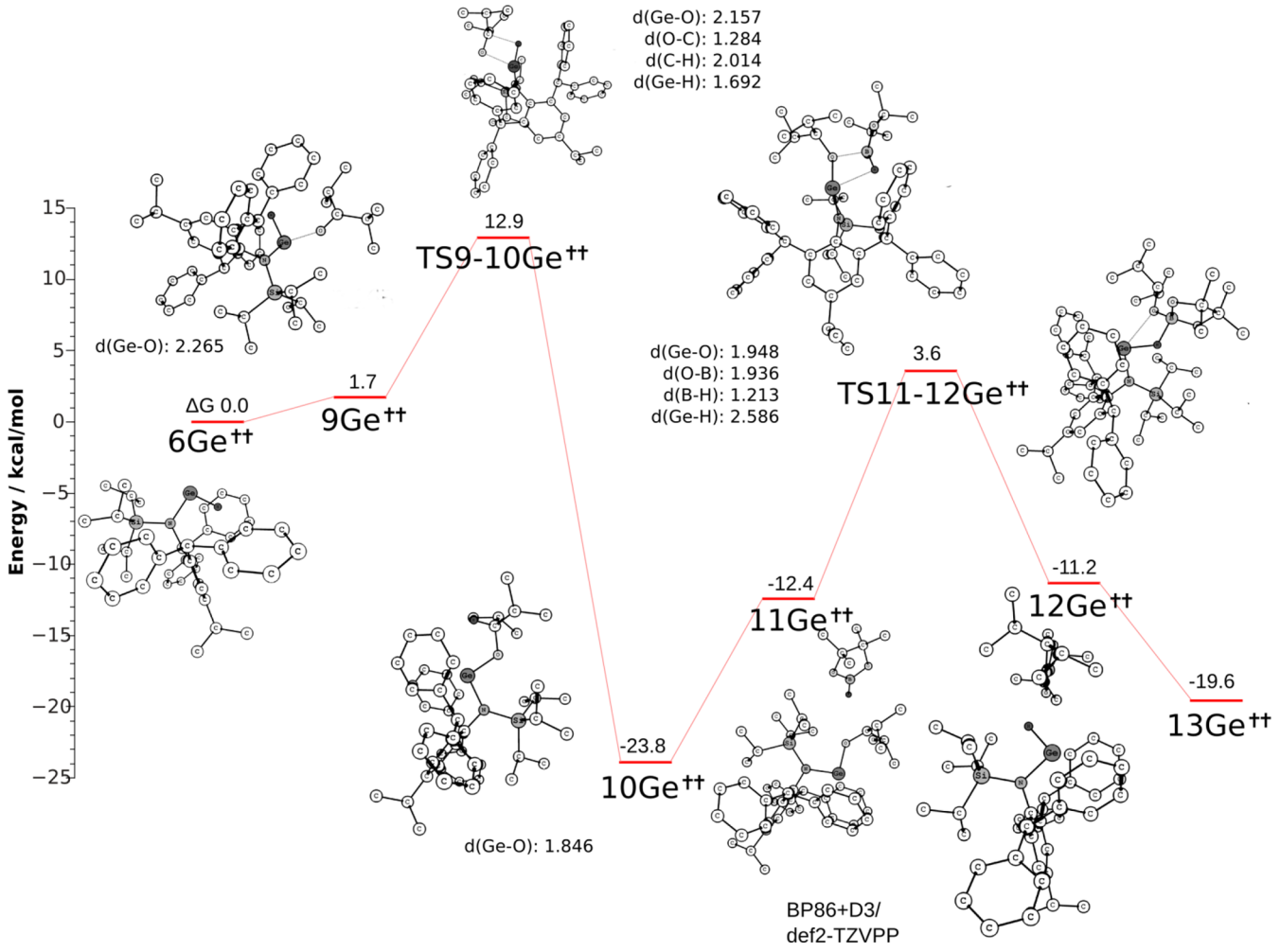

Figure 7. Calculated BP86+D(BJ)/def2-TZVPP reaction profile for the reaction of $O{=}C(Pr^i)_2$ with HBpin, catalyzed with **6Ge**††. Bond lengths are given in angstroms and angles in degrees.[14]

the carbonyl moiety of $O{=}C(Pr^i)_2$, yielding **10M**††. The hydridotetrylation reactions have rather low barriers and are exergonic by ΔG°_{298} = −23.8 kcal/mol (M = Ge) and ΔG°_{298} = −16.7 kcal/mol (M = Sn). The second part of the reactions involves σ-bond metathesis, which is the rate-determining step for each process. The activation barrier for the hydridogermylene-catalyzed σ-bond metathesis that gives **13M**†† as the final product is clearly higher ($\Delta G^{\circ\ddagger}_{298}$ = 27.4 kcal/mol) than that for the hydridostannylene-catalyzed process ($\Delta G^{\circ\ddagger}_{298}$ = 16.1 kcal/mol). Calculations suggest that the latter reaction step is exergonic by ΔG°_{298} = −3.4 kcal/mol, while the former reaction is endergonic by ΔG°_{298} = 4.2 kcal/mol. Both reactions are experimentally observed, which means that either the thermodynamics of the reactions are not correctly described at this level of theory or the products are further stabilized.

5. REACTION WITH CO_2

The singly bonded amidodigermyne **1Ge** where L† = NAr*-($SiMe_3$) (Ar* = $C_6H_2\{C(H)Ph_2\}_2Me$-2,6,4) proved not only to react rapidly with H_2[9] but also to react with CO_2 at temperatures as low as −40 °C.[11] The reaction is not a simple addition of CO_2 but a reduction of CO_2 to CO. The mechanism of the reaction was elucidated with quantum-chemical calculations. Figure 9 shows the calculated reaction profile for the reaction of **1Ge** with CO_2.

The initial step of the three-step reaction exhibits the unusual situation that there are two different transition states, **TS1a** and **TS1b**, that connect the educt **1Ge** + CO_2 and the first intermediate **IM1**. The transition states involve a side-on approach of the CO_2 molecule to one (**TS1a**) or both (**TS1b**) germanium centers, which show distinctively different Ge−Ge distances. The activation energy of **TS1a** ($\Delta G^{\circ\ddagger}_{298}$ = 17.0 kcal/mol) is smaller than that of **TS1b** ($\Delta G^{\circ\ddagger}_{298}$ = 22.2 kcal/mol). Intrinsic reaction coordinate calculations proved that **TS1a** and **TS1b** are indeed transition states for the same reaction step and not for consecutive reactions via another intermediate.[11] The compound **IM1** then rearranges with a low barrier (**TS2**, $\Delta G^{\circ\ddagger}_{298}$ = 4.1 kcal/mol), yielding the *trans*-germacarboxylatogermanium(II) amide complex **IM2**, which is 5.0 kcal/mol lower in energy than **IM1**. The reaction up to this point is weakly exergonic by ΔG°_{298} = −4.5 kcal/mol. The final step of the reaction, which has an activation energy (**TS3**, $\Delta G^{\circ\ddagger}_{298}$ = 16.3 kcal/mol) similar to that of the initial process, involves CO elimination, which is clearly exergonic by ΔG°_{298} = −13.2 kcal/mol. The calculated reaction profile is in good agreement with experiment. The final product **13Ge** has been isolated and structurally characterized by X-ray analysis, while the intermediate **IM2** was identified by comparing the recorded NMR signals with those in the calculated spectrum.[11]

dx.doi.org/10.1021/ic500457q | Inorg. Chem. 2014, 53, 6482−6490

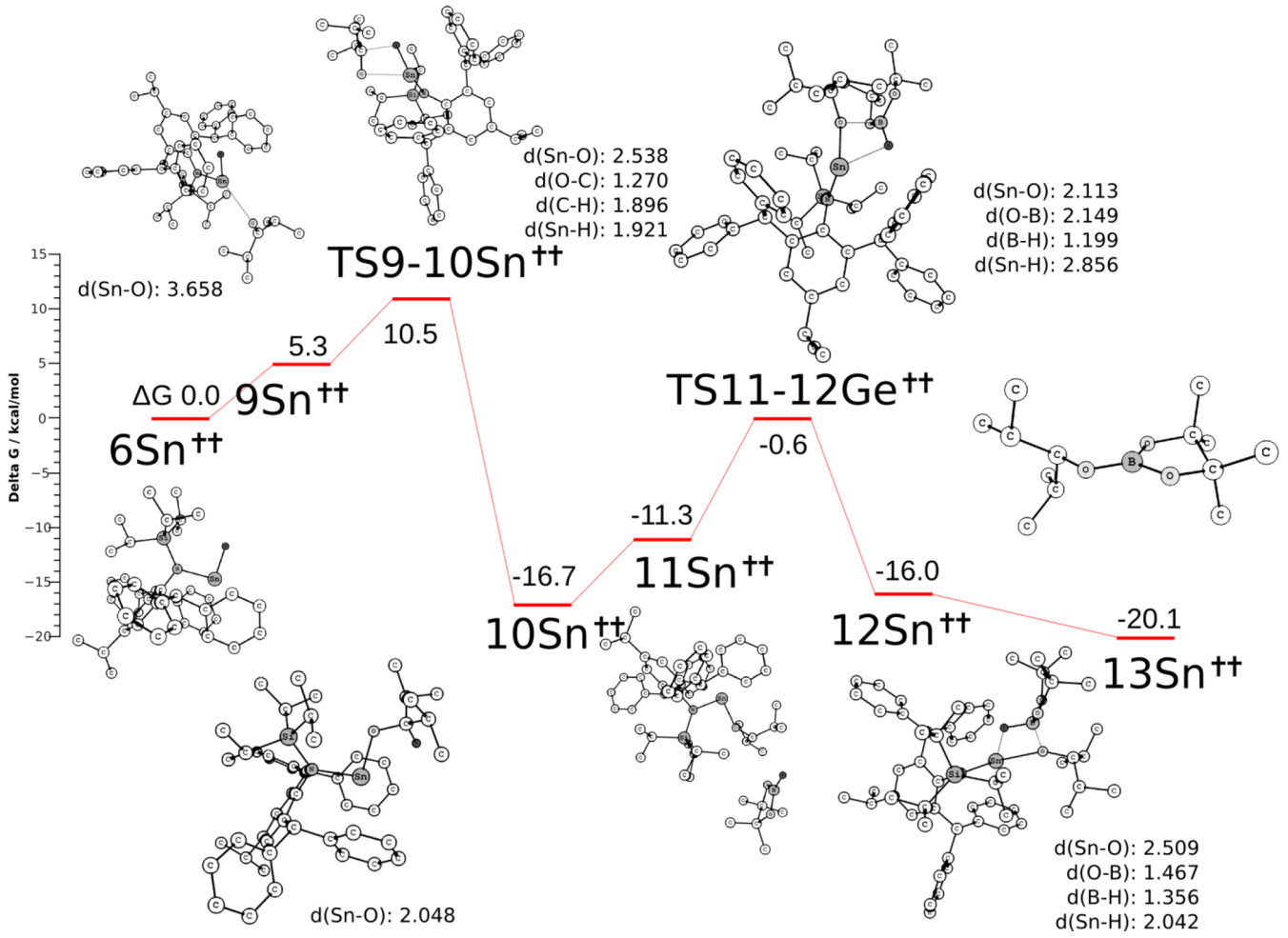

Figure 8. Calculated BP86+D(BJ)/def2-TZVPP reaction profile for the reaction of O═C(Pr^{i})$_2$ with HBpin, catalyzed with **6Sn**††. Bond lengths are given in angstroms and angles in degrees.

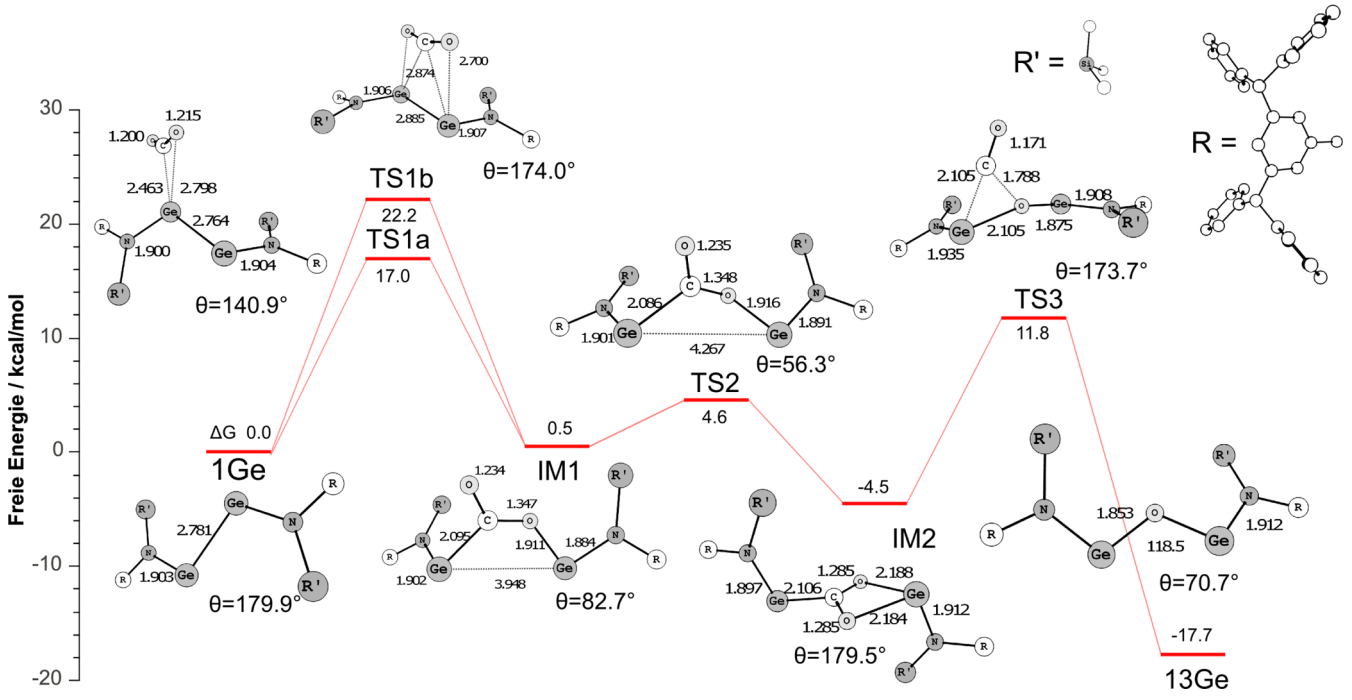

Figure 9. Calculated reaction profile for the reaction of **1Ge** with CO_2 (BP86-D3/def2-TZVPP//BP86/def2-SVP). Bond lengths are given in angstroms and angles in degrees. The dihedral angle θ refers to the NGeGeN fragment.[11]

dx.doi.org/10.1021/ic500457q | Inorg. Chem. 2014, 53, 6482−6490

6. SUMMARY AND CONCLUSION

The quantum theoretical results that are presented and discussed in this article emphasize the great value of the cooperation between theory and experiment in the search of new catalysts for the activation of small molecules. The calculated reaction profiles for the addition of H_2 and CO_2 to amidoditetrylynes and for the borylation of a ketone catalyzed by hydridogermylenes and hydridostannylenes provide insight into the experimentally observed processes. Apart from understanding the details of the reactions, the calculated data are very useful as a guideline for future experiments that can focus on more promising systems. At the same time, the experimental results show the limitations and accuracy of the theoretical methods, which are subject to ongoing improvements.

AUTHOR INFORMATION

Corresponding Authors

*E-mail: cameron.jones@monash.edu. Tel: +61-(0)3-9902-0391. Fax: +61-(0)3-9905-4597.

*E-mail: frenking@chemie.uni-marburg.de. Tel: +49-6421-282-5563. Fax: +49-6421-282-5566.

Notes

The authors declare no competing financial interest.

ACKNOWLEDGMENTS

This work was financially supported by the Deutsche Forschungsgemeinschaft and Australian Research Council.

REFERENCES

(1) Selected recent reviews: (a) Power, P. P. *Acc. Chem. Res.* **2011**, *44*, 627. (b) Asay, M.; Jones, C.; Driess, M. *Chem. Rev.* **2011**, *111*, 354. (c) Yao, S.; Xiong, Y.; Driess, M. *Organometallics* **2011**, *30*, 1748. (d) Power, P. P. *Nature* **2010**, *463*, 171. (e) Fischer, R. C.; Power, P. P. *Chem. Rev.* **2010**, *110*, 3877. (f) Schnöckel, H. *Chem. Rev.* **2010**, *110*, 4125. (g) Lee, V. Y.; Sekiguchi, A. *Organometallic Compounds of Low-Coordinate Si, Ge, Sn and Pb*; Wiley: Chichester, U.K., 2010.

(2) Power, P. P. *Chem. Rec.* **2012**, *12*, 238 See also refs 1a and 1d.

(3) (a) Pu, L.; Twamley, B.; Power, P. P. *J. Am. Chem. Soc.* **2000**, *122*, 3524. (b) Phillips, A. D.; Wright, R. J.; Olmstead, M. M.; Power, P. P. *J. Am. Chem. Soc.* **2002**, *124*, 5930. (c) Stender, M.; Phillips, A. D.; Wright, R. J.; Power, P. P. *Angew. Chem.* **2002**, *114*, 1863.

(4) (a) Sekiguchi, A.; Kinjo, R.; Ichinohe, M. *Science* **2004**, *305*, 1755. (b) Disilylynes were previously synthesized but could not be characterized by X-ray analysis by: Wiberg, N.; Niedermayer, W.; Fischer, G.; Nöth, H.; Suter, M. *Eur. J. Inorg. Chem.* **2002**, 1066. (c) Wiberg, N.; Vasisht, S. K.; Fischer, G.; Mayer, P. *Z. Allg. Anorg. Chem.* **2004**, *630*, 1823.

(5) Selected examples: (a) Takagi, N.; Nagase, S. *Organometallics* **2007**, *26*, 3627. (b) Lein, M.; Krapp, A.; Frenking, G. *J. Am. Chem. Soc.* **2005**, *127*, 6290. (c) Bridgeman, A. J.; Ireland, L. R. *Polyhedron* **2001**, *20*, 2841. (d) Chen, Y.; Hartmann, M.; Diedenhofen, M.; Frenking, G. *Angew. Chem., Int. Ed.* **2001**, *40*, 2052.

(6) Spikes, G. H.; Fettinger, J. C.; Power, P. P. *J. Am. Chem. Soc.* **2005**, *127*, 12232.

(7) Peng, Y.; Brynda, M.; Ellis, B. D.; Fettinger, J. C.; Rivard, E.; Power, P. P. *Chem. Commun.* **2008**, 6041.

(8) Zhao, L. L.; Huang, F.; Lu, G.; Wang, Z.-X.; Schleyer, P. v. R. *J. Am. Chem. Soc.* **2012**, *134*, 8856.

(9) Li, J.; Schenk, C.; Goedecke, C.; Frenking, G.; Jones, C. *J. Am. Chem. Soc.* **2011**, *133*, 18622.

(10) Li, J.; Stasch, A.; Schenk, C.; Jones, C. *Dalton Trans.* **2011**, *40*, 10448.

(11) Li, J.; Hermann, M.; Frenking, G.; Jones, C. *Angew. Chem., Int. Ed.* **2012**, *51*, 8611.

(12) Hermann, M.; Goedecke, C.; Frenking, G.; Jones, C. *Organometallics* **2013**, *32*, 6666.

(13) Hadlington, T. J.; Hermann, M.; Li, J.; Frenking, G.; Jones, C. *Angew. Chem., Int. Ed.* **2013**, *52*, 10199.

(14) Hadlington, T. J.; Hermann, M.; Li, J.; Frenking, G.; Jones, C. *J. Am. Chem. Soc.* **2014**, *136*, 3028.

(15) Frisch, M. J.; Trucks, G. W.; Schlegel, H. B.; Scuseria, G. E.; Robb, M. A.; Cheeseman, J. R.; Scalmani, G.; Barone, V.; Mennucci, B.; Petersson, G. A.; Nakatsuji, H.; Caricato, M.; Li, X.; Hratchian, H. P.; Izmaylov, A. F.; Bloino, J.; Zheng, G.; Sonnenberg, J. L.; Hada, M.; Ehara, M.; Toyota, K.; Fukuda, R.; Hasegawa, J.; Ishida, M.; Nakajima, T.; Honda, Y.; Kitao, O.; Nakai, H.; Vreven, T.; Montgomery, J. A., Jr.; Peralta, J. E.; Ogliaro, F.; Bearpark, M.; Heyd, J. J.; Brothers, E.; Kudin, K. N.; Staroverov, V. N.; Kobayashi, R.; Normand, J.; Raghavachari, K.; Rendell, A.; Burant, J. C.; Iyengar, S. S.; Tomasi, J.; Cossi, M.; Rega, N.; Millam, N. J.; Klene, M.; Knox, J. E.; Cross, J. B.; Bakken, V.; Adamo, C.; Jaramillo, J.; Gomperts, R.; Stratmann, R. E.; Yazyev, O.; Austin, A. J.; Cammi, R.; Pomelli, C.; Ochterski, J. W.; Martin, R. L.; Morokuma, K.; Zakrzewski, V. G.; Voth, G. A.; Salvador, P.; Dannenberg, J. J.; Dapprich, S.; Daniels, A. D.; Farkas, O.; Foresman, J. B.; Ortiz, J. V.; Cioslowski, J.; Fox, D. J. *Gaussian 09*, revision C.01; Gaussian, Inc.: Wallingford, CT, 2009.

(16) Turbomole 6.4, a development of University of Karlsruhe and Forschungszentrum Karlsruhe GmbH, 1989−2007, TURBOMOLE GmbH, since 2007, available from www.turbomole.com.

(17) (a) Becke, A. D. *Phys. Rev. A* **1988**, *38*, 3098. (b) Perdew, J. P. *Phys. Rev. B* **1986**, *33*, 8822.

(18) (a) Weigend, F.; Häser, M.; Patzelt, H.; Ahlrichs, R. *Chem. Phys. Lett.* **1998**, *294*, 143. (b) Weigend, F.; Ahlrichs, R. *Phys. Chem. Chem. Phys.* **2005**, *7*, 3297.

(19) Schäfer, A.; Horn, H.; Ahlrichs, R. *J. Chem. Phys.* **1992**, *97*, 2571.

(20) Metz, B.; Stoll, H.; Dolg, M. *J. Chem. Phys.* **2000**, *113*, 2563.

(21) Grimme, S.; Antony, J.; Ehrlich, S.; Krieg, H. *J. Chem. Phys.* **2010**, *132*, 154104.

(22) Klamt, A.; Schüürmann, G. *J. Chem. Soc., Perkin Trans.* **1993**, *2*, 799.

(23) Mitoraj, M. P.; Michalak, A.; Ziegler, T. *J. Chem. Theory Comput.* **2009**, *5*, 962.

(24) Ziegler, T.; Rauk, A. *Theor. Chim. Acta* **1977**, *46*, 1.

(25) Mitoraj, M. P.; Michalak, A. *J. Mol. Model.* **2007**, *13*, 347.

(26) Snijders, J. G.; Baerends, E. J.; Vernoojs, P. *At. Data Nucl. Data Tables* **1982**, *26*, 483.

(27) te Velde, G.; Bickelhaupt, F. M.; Baerends, E. J.; Fonseca Guerra, C.; van Gisbergen, S. J. A.; Snijders, J. G.; Ziegler, T. *J. Comput. Chem.* **2001**, *22*, 931.

(28) Zhao, Y.; Truhlar, D. G. *Theor. Chem. Acc.* **2008**, *120*, 215.

(29) Neese, F. *WIREs Comput. Mol. Sci.* **2012**, *2*, 73.